Experimental Observation of One-Dimensional Superradiance Lattices in Ultracold Atoms

Liangchao Chen,[1,2] Pengjun Wang,[1,2,*] Zengming Meng,[1,2] Lianghui Huang,[1,2] Han Cai,[3,4,†]
Da-Wei Wang,[3,6] Shi-Yao Zhu,[3,5] and Jing Zhang[1,5,‡]

[1]*State Key Laboratory of Quantum Optics and Quantum Optics Devices, Institute of Opto-Electronics, Shanxi University, Taiyuan 030006, People's Republic of China*
[2]*Collaborative Innovation Center of Extreme Optics, Shanxi University, Taiyuan 030006, People's Republic of China*
[3]*Interdisciplinary Center of Quantum Information and Department of Physics, Zhejiang University, Hangzhou 310027, People's Republic of China*
[4]*Institute of Quantum Science and Engineering, Texas A&M University, College Station, Texas 77843, USA*
[5]*Synergetic Innovation Center of Quantum Information and Quantum Physics, University of Science and Technology of China, Hefei, Anhui 230026, People's Republic of China*
[6]*CAS Center of Excellence in Topological Quantum Computation, University of Chinese Academy of Sciences, Beijing 100190, People's Republic of China*

We measure the superradiant emission in a one-dimensional (1D) superradiance lattice (SL) in ultracold atoms. Resonantly excited to a superradiant state, the atoms are further coupled to other collectively excited states, which form a 1D SL. The directional emission of one of the superradiant excited states in the 1D SL is measured. The emission spectra depend on the band structure, which can be controlled by the frequency and intensity of the coupling laser fields. This work provides a platform for investigating the collective Lamb shift of resonantly excited superradiant states in Bose-Einstein condensates and paves the way for realizing higher dimensional superradiance lattices.

Ultracold atoms have been a highly controllable system for investigating condensed matter physics [1] and providing versatile applications in quantum optics and quantum information processing [2]. In addition to absorption imaging [3], light scattering is a common method for observing and analyzing physics in cold atoms, such as the optical Bragg scattering of cold atomic gases [4–7] and the antiferromagnetic correlations in a Fermi-Hubbard model [8]. Different from the optical Bragg scattering with hot atoms [9–12], highly coherent atomic matter waves are usually involved in cold atoms [13]. Superradiance [14] is also important in studying collective effect in atoms [15–17]. In Bose-Einstein condensates (BEC) off-resonant pumping fields are usually used, such as the BEC superradiance in a free space [18] and the superradiance phase transition in an optical cavity [19]. Dipolar interactions induced by off-resonant light in BEC can result in rotons [20] and Cooper pairs [21], which have a substantial effect on the excitation spectra of the BEC [22]. Off-resonant fields are also used to investigate the collective effect in the superradiance of noncondensed cold atoms [23,24].

BEC superradiance with on-resonant pumping is more difficult to observe since the pumping field and the superradiant radiation are in the same direction. However, many interesting phenomena in superradiance and subradiance of the phase-correlated timed Dicke states [17,25–29] and the

collective Lamb shift [30–33] only happen when the superradiant states are near or on-resonantly excited. Recently, the superradiance lattice composed by timed Dicke states in momentum space was proposed in noncondensed atoms [34]. Since the direction of the emission of the superradiant states in the superradiance lattice can be different from that of the probe field, we are able to investigate the on-resonantly excited superradiant states in a BEC. In this Letter, we report the experimental realization of the superradiance lattice in a BEC of ^{87}Rb ultracold atoms. The light emitted by one of the superradiant states in the superradiance lattice is measured. Different from the well-known Bragg scattering of cold atoms with periodically modulated density [7], the spectra of the superradiant emission demonstrate the band structure of a one-dimensional tight-binding lattice.

To highlight the underlying physics, we consider a three-level Λ-type system with one excited state $|e\rangle$ and two ground states $|g\rangle$ and $|m\rangle$. The atoms are initially prepared in a BEC of the ground state $|g\rangle$. We approximate this state as $|G\rangle \equiv |N, \mathbf{q} = 0\rangle_g$, which means N atoms in the state $|g\rangle$ with zero momentum $\mathbf{q}$. This is a good approximation for the current investigation although the atoms are in a trap and the ground state contains other momentum components. A single photon resonantly absorbed by the BEC results in the state $|1, \mathbf{k}_p\rangle_e |N - 1, 0\rangle_g$, where $\mathbf{k}_p$ is the wave vector of the probe photon; i.e., one atom is excited from

$|g\rangle$ to $|e\rangle$ and acquires a recoil momentum $\mathbf{k}_p$. We first analyze the spontaneous emission of this excited state. The interaction Hamiltonian between the atoms and the vacuum modes is ($\hbar = 1$)

$$H_1 = \sum_{\mathbf{k},\mathbf{q}} g_{\mathbf{k}} a_{\mathbf{k}}^{\dagger} b_g^{\dagger}(\mathbf{q}-\mathbf{k}) b_e(\mathbf{q}) + \text{H.c.}, \qquad (1)$$

where $a_{\mathbf{k}}$ is the annihilation operator of the photon with wave vector $\mathbf{k}$, $g_{\mathbf{k}}$ is the coupling constant between the photon and atoms, $b_i(\mathbf{q})$ is the annihilation operator of the atoms in the internal state $|i\rangle$ with momentum $\mathbf{q}$.

One particular vacuum mode with wave vector $\mathbf{k}_p$ dominates the spontaneous emission in the excited BEC. It is easy to find that the coupling between the single photon excited state $|1,\mathbf{k}_p\rangle_e |N-1,0\rangle_g$ and the ground state is

$$\langle 0,0|_e \langle N,0|_g H_1 |1,\mathbf{k}_p\rangle_e |N-1,0\rangle_g = \sqrt{N} g_{\mathbf{k}_p} a_{\mathbf{k}_p}^{\dagger}, \qquad (2)$$

accompanied by the radiation of a photon with wave vector $\mathbf{k}_p$. The interaction is enhanced by $\sqrt{N}$ times, which is a signature of the superradiance. Instead, if the atoms radiate a photon with momentum $\mathbf{k} \neq \mathbf{k}_p$, the coupling strength is

$$\langle 0,0|_e \langle 1,\mathbf{k}_p - \mathbf{k}; N-1,0|_g H_1 |1,\mathbf{k}_p\rangle_e |N-1,0\rangle_g = g_{\mathbf{k}} a_{\mathbf{k}}^{\dagger}. \qquad (3)$$

Here $\langle 1, \mathbf{k}_p - \mathbf{k}; N-1, 0|_g$ denotes the final state bra with one atom with momentum $\mathbf{k}_p - \mathbf{k}$ and $N-1$ atoms with zero momentum in the state $|g\rangle$. Therefore, the spontaneous decay of the state $|1,\mathbf{k}_p\rangle_e |N-1,0\rangle_g$ is dominated by the superradiance emission in the mode $\mathbf{k}_p$. The state $|1,\mathbf{k}_p\rangle_e |N-1,0\rangle_g$ is a BEC version of the timed Dicke state $|e_{\mathbf{k}_p}\rangle = (1/\sqrt{N}) \sum_j e^{i\mathbf{k}_p \cdot \mathbf{r}_j} |g_1, g_2, ..., e_j, ..., g_N\rangle$ [25], where $|i_j\rangle$ ($i = e, g$) and $\mathbf{r}_j$ are the internal states and position of the jth atom.

However, such a radiation is difficult to observe in experiments since the excitation and radiation signals are in the same direction. In order to observe the directional radiation, we need to change the wave vector of the excited state. This can be done by introducing two coherent fields that drive the transition between the excited state $|e\rangle$ and another ground state $|m\rangle$. The interaction Hamiltonian is

$$H_c = \sum_{\mathbf{q},j} \Omega_j b_m^{\dagger}(\mathbf{q}-\mathbf{k}_{cj}) b_e(\mathbf{q}) + \text{H.c.}, \qquad (4)$$

where Ω_j are the Rabi frequencies of the coupling fields with the wave vectors $\mathbf{k}_{cj}$ ($j = 1, 2$). We introduce a short-hand notation $|e_l\rangle \equiv |1,\mathbf{k}_l\rangle_e |N-1,0\rangle_g$ and $|m_l\rangle \equiv |1,\mathbf{k}_l - \mathbf{k}_{c1}\rangle_m |N-1,0\rangle_g$ with $\mathbf{k}_l = \mathbf{k}_p - l(\mathbf{k}_{c1} - \mathbf{k}_{c2})$ and l an integer. Through the Hamiltonian in Eq. (4), $|e_l\rangle$ and $|m_l\rangle$ form a 1D tight-binding chain, as shown in Fig. 1(a). Considering the on-site potential induced by the detuning of the coupling field $\Delta_c \equiv \nu_c - \omega_{em}$ with ν_c the coupling field frequency and ω_{em} the transition frequency between $|e\rangle$ and $|m\rangle$, we can write down the interaction
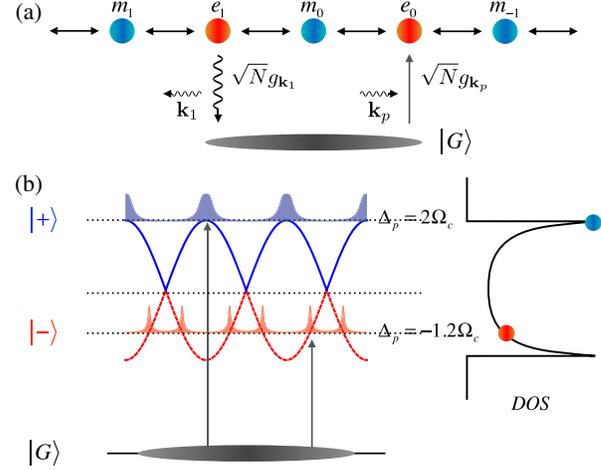

FIG. 1. Band structure of the superradiance lattice in BEC. (a) In the superradiance lattice, the pump laser populates $|e_0\rangle$, which is a superradiant state and coupled to other collective states. Among these states, only $|e_1\rangle$ is superradiantly coupled to the ground states and its directional emission is measured. (b) The atoms dressed by the standing wave have different energies of their eigenstates $|\pm\rangle = (|e\rangle \pm |m\rangle)/\sqrt{2}$ at different positions. The excitation probabilities of the BEC atoms at different positions is plotted for two different pump frequencies. The total excitation probabilities are proportional to the density of states of a tight-binding model of collectively excited states.

Hamiltonian in the subspace expanded by $|e_l\rangle$ and $|m_l\rangle$ in a tight-binding form,

$$H_I = \sum_l \frac{\Delta_c}{2} (|m_l\rangle\langle m_l| - |e_l\rangle\langle e_l|)$$
$$+ (\Omega_1 |m_l\rangle\langle e_l| + \Omega_2 |m_{l-1}\rangle\langle e_l| + \text{H.c.}). \qquad (5)$$

In this lattice, if $|\mathbf{k}_f| = |\mathbf{k}_p|$ for a certain $|e_f\rangle$, a vacuum mode with wave vector $\mathbf{k}_f$ can couple the excited state $|e_f\rangle$ back to the ground state via directional superradiant emission in $\mathbf{k}_f$. Other states with $|\mathbf{k}_l| \neq |\mathbf{k}_p|$ cannot find a vacuum mode to achieve a superradiant enhancement in their spontaneous emission. The kinetic energy due to the recoil can be neglected (see the Supplemental Material [35]). In our experiment, $f = 1$, as shown in Fig. 1(a) and the radiation of $|e_1\rangle$ is detected.

A pure BEC with typically 5×10^5 ^{87}Rb atoms is prepared in the $|g\rangle \equiv |F = 2, m_F = 2\rangle$ hyperfine ground state sublevel confined in a cross-beam dipole trap at a wavelength near 1064 nm. The geometric mean of the trapping frequencies is $\bar{\omega} \simeq 2\pi \times 80$ Hz. The atomic size is estimated in the Thomas-Fermi regime to be 20 μm, when the scattering length for $|g\rangle$ state at zero magnetic field is about $100 a_0$. The D_1 line (around 795 nm) of ^{87}Rb atom is considered as a simple three-level Λ-type model as shown in Fig. 2(a) due to the large hyperfine splitting of 816.8 MHz between the two excited states. We choose the

other two relevant hyperfine levels $|e\rangle \equiv |F' = 1, m'_F = 1\rangle$, $|m\rangle \equiv |F = 1, m_F = 1\rangle$. A homogeneous bias magnetic field along the z axis (gravity direction) is provided with $B_0 = 0.6$ G by a pair of coils operating in the Helmholtz configuration. A pair of strong coupling laser beams with the intersecting angle $\theta = 48°$ drive the transition between $|e\rangle$ and $|m\rangle$, as shown in Fig. 2(b). The coupling laser beams have the waist ($1/e^2$ radius) about 280 μm at the position of the BEC. The standing wave pattern formed by the coupling fields have about 20 periods in the atomic gases. A weak probe laser used to pump the atoms from $|g\rangle$ to $|e\rangle$ has a waist about 600 μm. The frequency locking and detuning of the coupling and probe lasers are described in the Supplemental Material [35]. The coupling and probe lasers illuminate atoms simultaneously with 20 μs. The intersecting angle between the superradiant emission and the probe light is about $\phi \sim 180° - \theta = 132°$. In order to obtain the dark background and high signal-noise ratio for detecting the superradiant emission, the intersecting angle between the plane of the two coupling beams and the plane of the probe-superradiant beams is $\varphi = 11°$, as shown in Fig. 2(b). The resulting superradiant emission is measured with an EMCCD.

If we only have one coupling laser, the two states $|e_0\rangle$ and $|m_0\rangle$ and the ground state form an EIT configuration. Since the probe (pump) beam has a waist much larger than
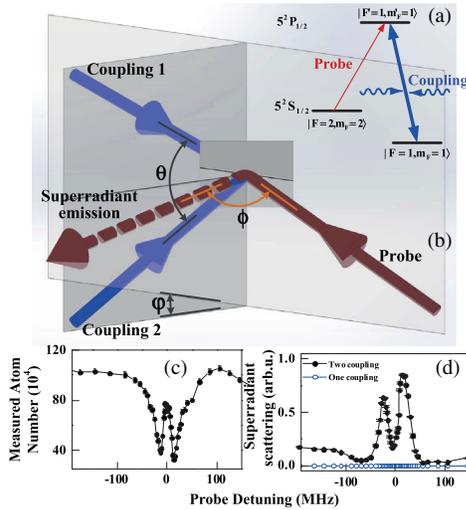
the coupling beams and the size of the BEC, we measure the remaining atoms by the time of flight absorption image after turning on the coupling and probe pulse for 20 μs, rather than measure the transmitted probe beam. Figure 2(c) shows a transparency window at the center. As a comparison to the latter experiment with two coupling beams, the superradiant emission in this case is measured to be zero, as shown in Fig. 2(d) (empty circles). In contrast, the solid dots in Fig. 2(d) show a typical superradiant emission when we have two coupling lasers. Two peaks due to the density of states (DOS) of the 1D tight-binding lattice [see Fig. 1 (a)] were observed.

The superradiance lattice band structure can be easily tuned by the laser parameters. For instance, the band gap can be opened by tuning the detunings of the coupling fields from the atomic transition frequency between $|e\rangle$ and $|m\rangle$. The bandwidth can be tuned by the laser intensities of the coupling laser field. The superradiant emission from the state $|e_1\rangle$ depends on this band structure. The probability that the superradiance lattice gets excited is roughly proportional to the DOS at the probe field frequency [as shown in Fig. 1(a)], characterized by the two peaks at the end of the spectra. The excitation has a periodic structure in position space, which means that it contains discrete momentum components. One of these components is the superradiant excited state $|e_1\rangle$, which inherits the two-peak feature of the DOS, as shown for different coupling field strengths in Fig. 3(a). Since the bandwidth is $4\Omega_c$, where $\Omega_c = \Omega_1 = \Omega_2$, the separation between the two peaks gets larger when we increase the coupling laser power. In Fig. 3(b) we plot the emission spectra for different detunings of the coupling fields. The

FIG. 2. Experimental configuration of the 1D superradiance lattice in BEC. (a) Energy diagram of the $5^2S_{1/2} - 5^2P_{1/2}$ transition of ^{87}Rb. (b) The experimental geometry and the laser configuration. The three planes in the figure are the plane of the two coupling beams, the plane of the probe-superradiant beams, and the equal intensity plane of the coupling beams. (c) EIT spectrum by measuring the remaining atoms with only one coupling laser. The power of each coupling laser is 200 μW and on resonance ($\Delta_c = 0$). The power of the probe laser is 25 μW. (d) Intensity of the superradiant scattering with a pair of coupling lasers. Each of the coupling lasers is 200 μW and the other parameters are the same as in (c). The data points are simply connected.
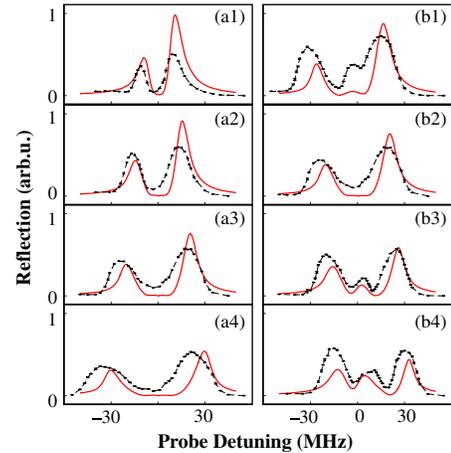

FIG. 3. Superradiant emission spectra for different intensities and detunings of the coupling laser. (a1)–(a4) The intensity of the coupling laser are (a1) 50, (a2) 100, (a3) 200, and (a4) 400 μW. The coupling laser is on resonance and the power of the probe light is 25 μW. (b1)–(b4). The detunings of the coupling laser are (b1) $\Delta_c = -10$, (b2) 0, (b3) 10, and (b4) 20 MHz. The powers of each coupling laser and the probe laser are 200 and 25 μW. The data points are simply connected with black lines and the red curves are the theoretical fitting.

coupling field detuning introduces an on-site potential in the superradiance lattice; i.e., the $|e_l\rangle$ and $|m_l\rangle$ states have an energy offset Δ_c, as shown in Eq. (5). This opens a band gap and introduces asymmetry of the $|e\rangle$ components in the two bands. When $\Delta_c > 0$ ($\Delta_c < 0$), the lower (upper) band contains more components of $|e\rangle$ states. Since the probe field only couples the ground state to the $|e\rangle$ component, the peak in the upper band gets higher compared with the other peak when we change Δ_c from positive to negative. A similar asymmetry was also predicted in four-wave mixing in two-level atoms [45]. The apparent third peaks in the middle of the spectra are due to the two dips at the one- and two-photon resonances. The dip at the two-photon resonance is due to the effect of EIT. At the one-photon resonance, the power of the coupling fields is not much larger and even smaller than that of the probe field, which induces absorption of the probe field without superradiant emission [35].

In the experiments, the right peak is generally higher than the left peak. Part of the reason for the asymmetry between the two peaks is attributed to the dispersion of the light field in BEC. The right peak can be tuned lower than the left peak by changing the angle of the incident probe field. This is similar to the phase matching in four-wave-mixing [11,46]. The spectra due to different angles of the incident probe beam is plotted in Fig. 4. Since the BEC is highly dispersive to the probe light near the EIT point, we must take into account the phase mismatch due to this dispersion, $\Delta k = 2[n(\nu_p)\nu_p \cos(\phi/2) - \nu_c \sin(\theta/2)]/c$,
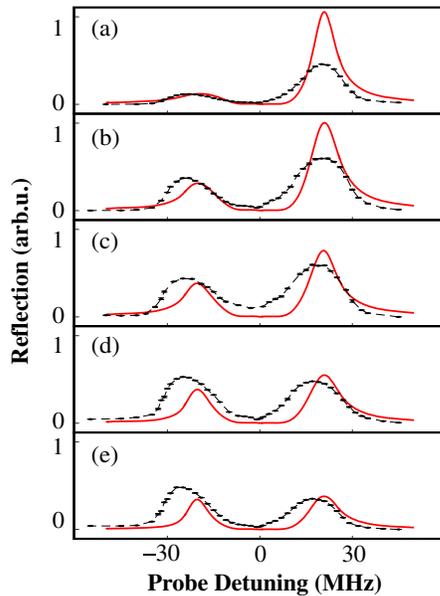

FIG. 4. Superradiant emission spectra for different incident angles of the incident probe beam. The deviation of the angle of the probe beam from $\phi = 132°$ are (a) $-0.9°$, (b) $-0.3°$, (c) $0°$, (d) $0.3°$, and (e) $0.6°$. The powers of each coupling laser is $200~\mu W$. The power of the probe light is $25~\mu W$. $\Delta_c = 0$. The data points are simply connected with black lines and the red curve is the theoretical fitting.

where ν_p and ν_c are the frequencies of the probe and coupling fields and n is the refraction index of the BEC. For fixed ϕ and θ, the phase mismatch Δk is basically linear to the probe detuning across the single photon resonance of the probe field. The peak that has smaller phase mismatch is higher than the other peak.

The asymmetry observed in the experiment cannot be fully explained by the dispersion in our current model [35]. The two peaks are generally shifted to the low frequency side. This can be attributed to two factors that are not taken into account in the current theoretical model. One is the nonzero momentum states in the BEC due to the trapping and interaction between atoms. The other is the collective decay rate and Lamb shift of the superradiant states [30]. A detailed calculation of these two quantities in the current experiment is difficult due to the near resonance condition [21,47].

The superradiant emission with a standing-wave coupled three-level EIT configuration is different from the ordinary Bragg scattering [7,48] or the degenerate four-wave mixing [49] from an ensemble of density modulated cold atoms, where only two atomic levels are relevant. In those cases, the standing wave forms an optical lattice that modulates the density of the atomic ensemble, such that the refractive index of the probe beam is periodically modulated and a photonic crystal is formed. The reflection spectra demonstrate the band structure of a photonic crystal. Although some density modulation might still exist in our experiments, the reflection spectra specifically demonstrate the band structure of a momentum-space tight-binding lattice. Each state in this BEC superradiance lattice is analogous to the timed Dicke state [25] or the collective spin-wave excitation in the DLCZ protocol [50]. In the Supplemental Material [35], we have compared the results of the superradiance lattice in BEC and density modulation induced photonic crystal in BEC, as well as the results of BEC and noncondensed cold atoms.

In conclusion, we have shown the superradiance spectra of a one-dimensional superradiance lattice with ultracold ^{87}Rb atoms. The relation between the spectra and the coupling field detuning and intensity can be explained by the band structure of the superradiance lattice. Many-body effect due to interactions between atoms might be responsible for the asymmetries in the spectra. The lattice can be generalized to two dimensions where the Haldane model can be simulated [51].

*pengjun_wang@sxu.edu.cn
†hancai@zju.edu.cn
‡jzhang74@sxu.edu.cn, jzhang74@yahoo.com

[1] M. Greiner, O. Mandel, T. Esslinger, T. W. Hansch, and I. Bloch, Nature (London) **415**, 39 (2002).

[2] I. Bloch, J. Dalibard, and W. Zwerger, Rev. Mod. Phys. **80**, 885 (2008).

[3] K. B. Davis, M.-O. Mewes, M. R. Andrews, N. J. van Druten, D. S. Durfee, D. M. Kurn, and W. Ketterle, Phys. Rev. Lett. **75**, 3969 (1995).

[4] G. Birkl, M. Gatzke, I. H. Deutsch, S. L. Rolston, and W. D. Phillips, Phys. Rev. Lett. **75**, 2823 (1995).

[5] M. Weidemuller, A. Hemmerich, A. Gorlitz, T. Esslinger, and T. W. Hansch, Phys. Rev. Lett. **75**, 4583 (1995).

[6] S. Slama, C. von Cube, B. Deh, A. Ludewig, C. Zimmermann, and Ph. W. Courteille, Phys. Rev. Lett. **94**, 193901 (2005).

[7] A. Schilke, C. Zimmermann, P. W. Courteille, and W. Guerin, Phys. Rev. Lett. **106**, 223903 (2011).

[8] R. A. Hart, P. M. Duarte, T. L. Yang, X. Liu, T. Paiva, E. Khatami, R. T. Scalettar, N. Trivedi, D. A. Huse, and R. G. Hulet, Nature (London) **519**, 211 (2015).

[9] M. Bajcsy, A. S. Zibrov, and M. D. Lukin, Nature (London) **426**, 638 (2003).

[10] I. H. Bae, H. S. Moon, M. K. Kim, L. Lee, and J. B. Kim, Appl. Opt. **47**, 4849 (2008).

[11] Y. P. Zhang, Z. G. Wang, Z. Q. Nie, C. B. Li, H. X. Chen, K. Q. Lu, and M. Xiao, Phys. Rev. Lett. **106**, 093904 (2011).

[12] D. W. Wang, H. T. Zhou, M. J. Guo, J. X. Zhang, J. Evers, and S. Y. Zhu, Phys. Rev. Lett. **110**, 093901 (2013).

[13] P. Meystre, Atom Optics (Springer-Verlag, New York, 2001).

[14] R. Dicke, Phys. Rev. **93**, 99 (1954).

[15] N. Skribanowitz, I. P. Herman, J. C. MacGillivray, and M. S. Feld, Phys. Rev. Lett. **30**, 309 (1973).

[16] R. G. DeVoe and R. G. Brewer, Phys. Rev. Lett. **76**, 2049 (1996).

[17] A. Goban, C.-L. Hung, J. D. Hood, S.-P. Yu, J. A. Muniz, O. Painter, and H. J. Kimble, Phys. Rev. Lett. **115**, 063601 (2015).

[18] S. Inouye, A. P. Chikkatur, D. M. Stamper-Kurn, J. Stenger, and W. Ketterle, Science **285**, 571 (1999).

[19] K. Baumann, C. Guerlin, F. Brennecke, and T. Esslinger, Nature (London) **464**, 1301 (2010).

[20] D. H. J. O'Dell, S. Giovanazzi, and G. Kurizki, Phys. Rev. Lett. **90**, 110402 (2003).

[21] W. Zhang, Phys. Lett. A **176**, 225 (1993).

[22] J. Steinhauer, R. Ozeri, N. Katz, and N. Davidson, Phys. Rev. Lett. **88**, 120407 (2002).

[23] M. O. Araujo, I. Kresic, R. Kaiser, and W. Guerin, Phys. Rev. Lett. **117**, 073002 (2016).

[24] S. J. Roof, K. J. Kemp, M. D. Havey, and I. M. Sokolov, Phys. Rev. Lett. **117**, 073003 (2016).

[25] M. O. Scully, E. S. Fry, C. H. Raymond Ooi, and K. Wodkiewicz, Phys. Rev. Lett. **96**, 010501 (2006).

[26] T. Bienaime, N. Piovella, and R. Kaiser, Phys. Rev. Lett. **108**, 123602 (2012).

[27] M. O. Scully, Phys. Rev. Lett. **115**, 243602 (2015).

[28] S. L. Bromley, B. Zhu, M. Bishof, X. Zhang, T. Bothwell, J. Schachenmayer, T. L. Nicholson, R. Kaiser, S. F. Yelin, M. D. Lukin, A. M. Rey, and J. Ye, Nat. Commun. **7**, 11039 (2016).

[29] W. Guerin, M. O. Araujo, and R. Kaiser, Phys. Rev. Lett. **116**, 083601 (2016).

[30] M. O. Scully, Phys. Rev. Lett. **102**, 143601 (2009).

[31] R. Röhlsberger, K. Schlage, B. Sahoo, S. Couet, and R. Rüffer, Science **328**, 1248 (2010).

[32] J. Keaveney, A. Sargsyan, U. Krohn, I. G. Hughes, D. Sarkisyan, and C. S. Adams, Phys. Rev. Lett. **108**, 173601 (2012).

[33] Z. Meir, O. Schwartz, E. Shahmoon, D. Oron, and R. Ozeri, Phys. Rev. Lett. **113**, 193002 (2014).

[34] D. W. Wang, R. B. Liu, S.-Y. Zhu, and M. O. Scully, Phys. Rev. Lett. **114**, 043602 (2015).

[35] See Supplemental Material at http://link.aps.org/supplemental/10.1103/PhysRevLett.120.193601 for the experimental setup and theoretical calculation and fitting for the experimental data, which includes Refs. [36–44].

[36] H. M. Price, T. Ozawa, and I. Carusotto, Phys. Rev. Lett. **113**, 190403 (2014).

[37] P. Wang, Z.-Q. Yu, Z. Fu, J. Miao, L. Huang, S. Chai, H. Zhai, and J. Zhang, Phys. Rev. Lett. **109**, 095301 (2012).

[38] L. W. Cheuk, A. T. Sommer, Z. Hadzibabic, T. Yefsah, W. S. Bakr, and M. W. Zwierlein, Phys. Rev. Lett. **109**, 095302 (2012).

[39] M. Ben Dahan, E. Peik, J. Reichel, Y. Castin, and C. Salomon, Phys. Rev. Lett. **76**, 4508 (1996).

[40] A. Polkovnikov, S. Sachdev, and S. M. Girvin, Phys. Rev. A **66**, 053607 (2002).

[41] C. Hooley and J. Quintanilla, Phys. Rev. Lett. **93**, 080404 (2004).

[42] Y.-J. Lin, K. Jiménez-García, and I. B. Spielman, Nature (London) **471**, 83 (2011).

[43] A. André and M. D. Lukin, Phys. Rev. Lett. **89**, 143602 (2002).

[44] B. W. Adams, J. Mod. Opt. **56**, 1974 (2009).

[45] H. Friedmann and A. D. Wilson-Gordon, Phys. Rev. A **57**, 4854 (1998).

[46] H. Kang, G. Hernandez, and Y. Zhu, Phys. Rev. A **70**, 061804 (2004).

[47] J. Javanainen, Phys. Rev. Lett. **75**, 1927 (1995).

[48] S. A. R. Horsley, J. H. Wu, M. Artoni, and G. C. La Rocca, Phys. Rev. Lett. **110**, 223602 (2013).

[49] G. L. Gattobigio, F. Michaud, J. Javaloyes, J. W. R. Tabosa, and R. Kaiser, Phys. Rev. A **74**, 043407 (2006).

[50] L. M. Duan, M. D. Lukin, J. I. Cirac, and P. Zoller, Nature (London) **414**, 413 (2001).

[51] D. W. Wang, H. Cai, L. Yuan, R. B. Liu, S.-Y. Zhu, and M. O. Scully, Optica **2**, 712 (2015).